Macromolecules

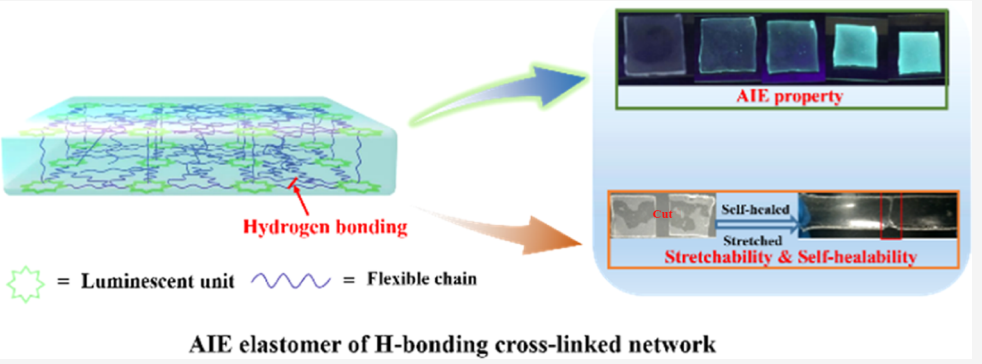
pubs.acs.org/Macromolecules Article

Stretchable and Self-Healing Elastomers with Aggregation-Induced Emission Based on Hydrogen Bonding Cross-Linked Networks

Yi Wan,[§] Xiang-Chun Li,[§] Jin Chen, Qian Wang, Chen Liu, Cheng-Fang Liu, and Wen-Yong Lai*

Cite This: https://doi.org/10.1021/acs.macromol.3c00088 Read Online

ACCESS | Metrics & More | Article Recommendations | Supporting Information



AIE elastomer of H-bonding cross-linked network

ABSTRACT: With the fast advancement of flexible and stretchable electronics, the development of organic semiconductors with intrinsic stretchability and self-healing properties is desirable and significant yet remains a substantial challenge. Herein, we propose a simple and effective synthetic strategy to construct intrinsically stretchable and self-healing organic light-emitting elastomers *via* incorporating aggregation-induced emission (AIE) luminogens into hydrogen-bonding cross-linked networks. Owing to the hydrogen-bonding interactions within the networks, the resulting light-emitting elastomers achieved a stress−strain of about 700% and a self-healing efficiency of over 70% under ambient conditions. More importantly, the resulting elastomers have been examined to be highly adhesive and compatible with the silver nanowire networks, exhibiting smart luminescence behaviors and excellent conductivity. This study sheds light on the design and development of stretchable and self-healing organic light-emitting elastomers with promising optoelectronic characteristics, which would inspire a wide range of fancy applications for flexible and stretchable electronics.

Downloaded via NANJING UNIV POSTS & TELECOM on April 21, 2023 at 14:05:04 (UTC).
See https://pubs.acs.org/sharingguidelines for options on how to legitimately share published articles.

INTRODUCTION

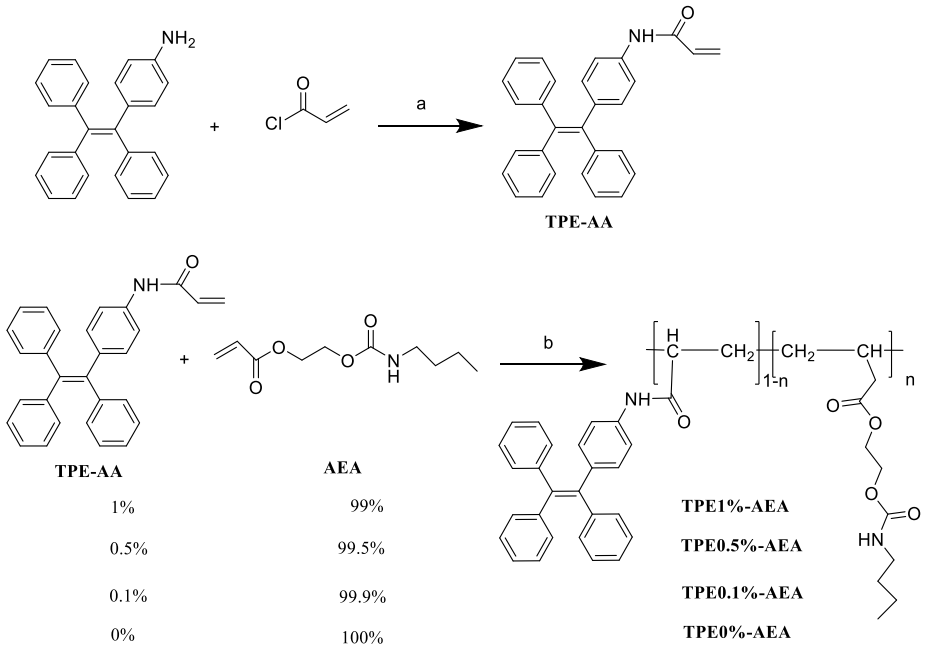
Over the past decades, organic optoelectronic materials have been extensively investigated for broad applications, *i.e.*, organic light-emitting diodes (OLEDs),[1−4] organic lasers,[5−7] and fluorescent sensors,[8−10] due to their attractive optoelectronic properties, intrinsic flexibility, and portability. Significant advances have been achieved in the design and development of high-performance organic semiconductors, and their optoelectronic properties have been greatly improved to be comparable to those of their inorganic counterparts.[11−16] However, most existing organic optoelectronic materials and their devices are susceptible to structural fractures under bending and may even suffer mechanical damage due to repetitive deformation or accidental cutting. Generally, these failures would seriously damage the optoelectronic performance of the devices, leading to the degradation of the device's performance or even being unusable.[17−19] It is desirable to develop organic optoelectronic materials and their devices that can maintain excellent optoelectronic properties in the presence of large deformations or even fractures.

Self-healing materials, inspired by the ability of human skin to repair itself after injury, are expected to tackle this issue. Self-healing materials with good mechanical properties can undergo large deformation and even autonomously repair physical damages with restored functionality.[20−24] In general, the healing mechanism of self-healing materials is induced by dynamic interactions, such as hydrogen bonding interactions,[25−27] metal−ligand coordination interactions,[28−30] ionic interactions,[31−33] host−guest interactions,[34,35] $\pi-\pi$ stacking interactions,[36,37] and reversible (dynamic) covalent bonds.[38−40] Although self-healing materials have been intensively investigated in the past decades, self-healing light-emitting materials as an important component of self-healing

Received: January 16, 2023
Revised: March 31, 2023

© XXXX American Chemical Society

Scheme 1. Synthetic Routes of TPE-AEA with a Different Molar Ratio of TPE Units[a]



[a]Conditions: (a) Et_3N, room temperature, 8 h and (b) 1-hydroxycyclohexyl phenyl ketone, ultraviolet light irradiation (365 nm, 400 W power), 6 h.

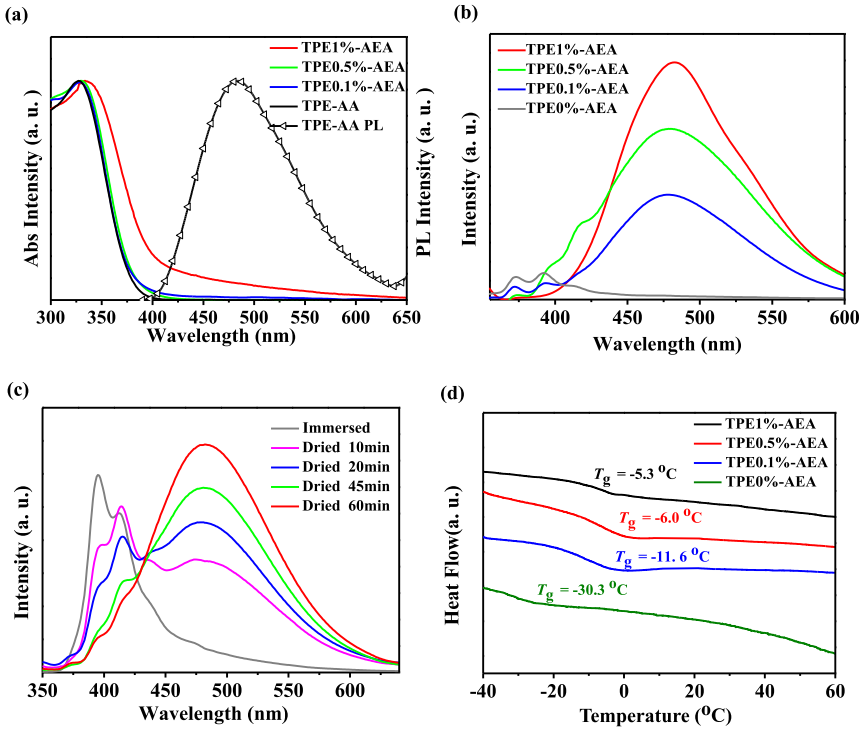


Figure 1. (a) UV−vis spectra of **TPE-AA** and **TPE-AEAs** and PL spectra of **TPE-AA** and (b) PL spectra of **TPE-AEAs** (λ_{ex} = 330 nm). (c) PL spectra of the methanol-immersed **TPE1%-AEA** elastomer after varying drying times at room temperature. (d) DSC curves of **TPE-AEA** elastomers. The measurements were carried out in a N_2 atmosphere with a heating rate of 10 °C/min.

optoelectronic devices have rarely been explored.[41] It would be exciting and ideal to develop flexible/stretchable electronics based on self-healing light-emitting materials with self-healing properties and good mechanical properties. However, there are still great challenges in the design and synthesis of the self-healing organic optoelectronic materials, especially for self-healing luminescent elastomers.

Herein, we present a simple approach to achieve self-healing luminescent elastomers based on hydrogen (H)-bonding cross-linked networks. The tetraphenyl ethylene (TPE) luminogen has been selected as the model luminescent units due to its high quantum efficiency and aggregation-induced emission (AIE) characteristics.[42,43] H-bonding cross-linked networks have been constructed to induce reversible self-healing

https://doi.org/10.1021/acs.macromol.3c00088
Macromolecules XXXX, XXX, XXX−XXX

processes with desirable spontaneous interactions, enabling the resulting materials to self-heal at ambient conditions. The main feature of this design is a simple and versatile synthesis process that enables the self-healing light-emitting semiconductors to be obtained by easily adjusting the ratio of the luminescent units to dynamic hydrogen bonding. Owing to accuracy design, the synthesized self-healing elastomers exhibited a strain capability of approximately 700% and a self-healing efficiency of over 70%. More importantly, the luminescence intensity did not significantly diminish when the elastomers were subjected to stress−strain or even fracture. Taking into account the aforementioned properties and the good elasticity of these materials, healable conductive composites based on the luminescent elastomers as the dielectric substrates were fabricated to realize a smart luminous process.

RESULTS AND DISCUSSION

As shown in Scheme 1, *N*-(4-(1,2,2-triphenylvinyl)phenyl)-acrylamide (**TPE-AA**) was synthesized by reacting 4-(1,2,2-triphenylvinyl)aniline with acrylyl chloride under appropriate conditions. The resulting **TPE-AA** was purified by silica gel column chromatography and characterized by ^{1}H NMR (Figure S1). Next, a series of TPE-based elastomers (**TPE-AEAs**) were synthesized through optically hinged reactions between 2-((butylcarbamoyl)oxy)ethyl acrylate (**AEA**) and **TPE-AA** with different molar percentages of **TPE-AA** of 2, 1, 0.5, 0.1, and 0 mol %, which were named **TPE2%-AEA**, **TPE1%-AEA**, **TPE0.5%-AEA**, **TPE0.1%-AEA**, and **TPE0%-AEA**, respectively. A series of TPE-based elastomers are shown in Figure S2. In the **TPE-AEA** system, the final product containing 2 mol % of TPE units hardly forms a regular elastomer compared to other elastomers, indicating poor modularity. The N−H, C═O, and NH−CO groups of these polymers (containing ≤1 mol % TPE units) were detected to confirm the hydrogen bonds by Fourier transform infrared spectroscopy (FTIR) (Figure S3).

To investigate the photophysical properties of **TPE-AA** and **TPE-AEAs**, their UV−vis absorption and photoluminescence (PL) spectra were recorded as depicted in Figures S4 and 1a,b. The UV−vis absorption and PL spectra of **TPE-AA** were measured in different volume fractions of the THF/H_2O mixed solvent. As shown in Figure S4, the absorption maximum shifted from 326 to 333 nm with the increase of water, probably due to the aggregation. In the PL spectra, **TPE-AA** presented typical AIE properties. By comparison, the aggregation induced by the addition of water significantly enhanced the PL intensity. The emission maximum shifted from 478 to 483 nm with the increase of water. In a mixed solvent of THF/H_2O = 1/99, the PL intensity was much higher than that in the dilute solution. These results indicate that **TPE-AA** could be used as an AIE cross-linker for the target elastomers. In UV−vis absorption spectra, the film of **TPE-AA** showed an absorption maximum at approximately 325 nm, which corresponded to the $\pi-\pi^*$ transition of the TPE units. **TPE0.1%-AEA**, **TPE0.5%-AEA**, and **TPE1%-AEA** showed maximum absorption at 330, 332, and 335 nm, respectively. The spectral red shift indicates that there is sufficient space between the side chains, which is caused by the backbone distortion due to steric hindrance of the side-chain polymer. As shown in Figure 1b, **TPE0.1%-AEA**, **TPE0.5%-AEA**, and **TPE1%-AEA** exhibited maximum emission at 485, 487, and 489 nm, respectively. The maximum emission peak appeared at 485−489 nm, which is consistent with the emission peak of the **TPE-AA** solid film. Moreover, PL spectra of **TPE1%-AEA** elastomers exhibited concentration-dependent behaviors. With the increase of TPE content, the PL emission intensity gradually increased. This result can be attributed to the increased density of the cross-linked side chains, which inhibits the rotation of the emitting molecules. As shown in Table 1, the photoluminescence quantum yields (PLQYs) of **TPE-AEAs** and **TPE-AA** were measured under ambient temperature. Notably, the PLQYs of all luminescent elastomers were close to that of **TPE-AA**, indicating that the introduction of abundant H-bonding side chains did not disrupt the inherent luminescent properties.

Table 1. Photophysical Properties of TPE-AEA Elastomers and TPE-AA

compounds	UV (nm)	PL (nm)	PLQY (%)
TPE1%-AEA	335	489	19.4
TPE0.5%-AEA	332	487	21.8
TPE0.1%-AEA	330	485	16.1
TPE0%-AEA			
TPE-AA	325	483	19.2

Besides, the PL response of all AIE elastomers against organic solvents was investigated in detail (Figure 1c). In this experiment, **TPE0.1%-AEA**, **TPE0.5%-AEA**, and **TPE1%-AEA** elastomers were immersed in methanol for 4 h. The PL spectra were measured with different drying times for investigating the PL response of elastomers against organic solvents. As a demonstration, the photographs of **TPE1%-AEA** immersed in methanol under 365 nm UV light after different drying times were recorded, as shown in Figure S5. The PL of **TPE1%-AEA** was easily quenched after methanol immersion, but the intensity of the AIE emission peak increased with drying time. Similar behaviors were observed for **TPE0.1%-AEA** and **TPE0.5%-AEA** elastomers (Figures S6, S7). These features may result from molecular motions around TPE units inside. Moreover, the immersion with organic solvents can effectively free the TPE units from the constraints of the H-bonding network.

To gain deep insights into the cross-linking degree, all obtained elastomers were measured by differential scanning calorimetry (DSC), and the results are depicted in Figure 1d. The glass transition temperatures (T_g) of **TPE1%-AEA**, **TPE0.5%-AEA**, and **TPE0.1%-AEA** were −5.3, −6.0, and −11.6 °C, respectively, which were significantly higher than that of **TPE0%-AEA** (−30.3 °C). The glass transition temperatures increased significantly with the increase of TPE units, demonstrating that the rigid TPE units could reduce the cross-linking density of H-bonds. In addition, the T_g values of **TPE-AEA** elastomers were all less than 0 °C, indicating that these elastomers have the self-healing ability at room temperature.

The mechanically tensile performance of all elastomers was measured at room temperature using strain−stress measurements. All elastomers exhibited good stretchable and self-healable properties owing to their H-bonding cross-linked network (Figure 2a). Figure 2b shows the stretching process of the **TPE1%-AEA** elastomer, indicating that it has good tensile properties. The stress−strain curves of pristine **TPE-AEA** elastomers are shown in Figure 2c. The **TPE0%-AEA** elastomer showed a maximum tensile stress of 0.35 MPa and a maximum tensile strain of 770%. With the increase of TPE

https://doi.org/10.1021/acs.macromol.3c00088
Macromolecules XXXX, XXX, XXX−XXX

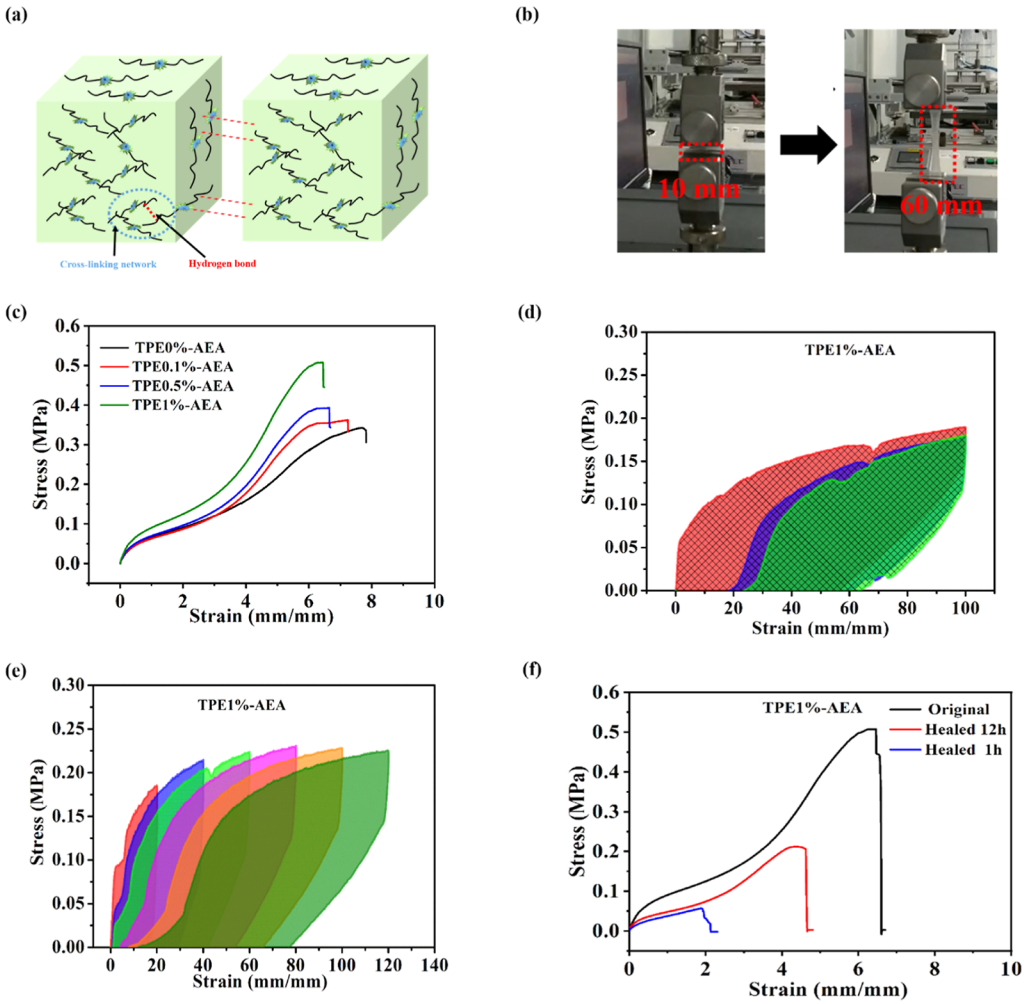


Figure 2. (a) Schematic illustration of luminescent elastomers based on H-bonding cross-linking networks; (b) photographs of stress-straining behaviors of the **TPE1%-AEA** elastomer; (c) stress−strain curves of the pristine **TPE-AEA** elastomers; and (d) continuous cycles of the **TPE1%-AEA** elastomer at a maximum strain of 100% (tensile rate: 50 mm/min), where red, blue, and green represent the first to third cycles; (e) cyclic cycles of the **TPE1%-AEA** elastomer at different strains (tensile rate: 50 mm/min), where red, blue, green, magenta, orange, and olive represent the first to the sixth cycles, and (f) stress−strain curves of the pristine **TPE1%-AEA** elastomer healed at room temperature over various times.

units, the maximum tensile stresses of **TPE0.1%-AEA**, **TPE0.5%-AEA**, and **TPE1%-AEA** were 0.37, 0.39, and 0.43 MPa, respectively, and the maximum tensile strain were 720, 660, and 645%, respectively. In addition, Young's modulus of **TPE-AEA** elastomers increased with the increase of the molar percentage of TPE units in the system. The results show that the stretchable capability of these elastomers can be adjusted by changing the proportion of cross-linked TPE units. The results of the elastic simulation of **TPE-AEA**s based on five hyperelastic models are shown in Figure S8. For **TPE-AEA**s, the sixth-order Ogden models and the simplified polynomial models simulate hyperelastic behavior and are closest to the test data for all tensile load ranges. All samples exhibit an inverse S-shaped stress−strain curve characteristic with a sharp increase in stress with strain beyond the elastic deformation region.[44,45] The **TPE1%-AEA** sample, for example, has a region of elastic deformation close to 120%, followed by a hardening of the material with increasing strain, and does not exhibit absolute plastic deformation.

The **TPE 1%-AEA** samples were studied, and their good elasticity and self-recovery properties were demonstrated by repeated cyclic tensile tests. As shown in Figure 4d, the sample was subjected to a maximum of 100% tension and then unloaded for three cycles, showing a clear hysteresis phenomenon. The sample produced the maximum dissipated energy (hysteresis loop area) in the first cycle, which decreased and gradually stabilized in the subsequent cycles, known as the Mullins effect. These observations suggest an accumulation of elastic deformation that is unlikely to relax to equilibrium within the time frame of a single cycle. Repeated stretching was also measured for various strains, as shown in Figure 4e. The results show that the **TPE1%-AEA** samples exhibited good self-recovery and elastic properties. Similar behaviors were observed for other elastomers, as depicted in Figure S9.

To study the self-healing capability of **TPE-AEA** elastomers, the prepared elastomers were cut into halves. The corresponding cut surfaces of the two halves were gently re-contacted under ambient conditions. After a period of time, the mechanical properties of these self-healing samples were characterized. The straining state of the **TPE1%-AEA** elastomer after healing for 12 h was recorded as shown in Figure S10. The strain−stress curves of the self-healed **TPE1%-AEA** elastomer at different healing times are depicted in Figure 2f. The stress−strain curves of other self-healed

https://doi.org/10.1021/acs.macromol.3c00088
Macromolecules XXXX, XXX, XXX−XXX

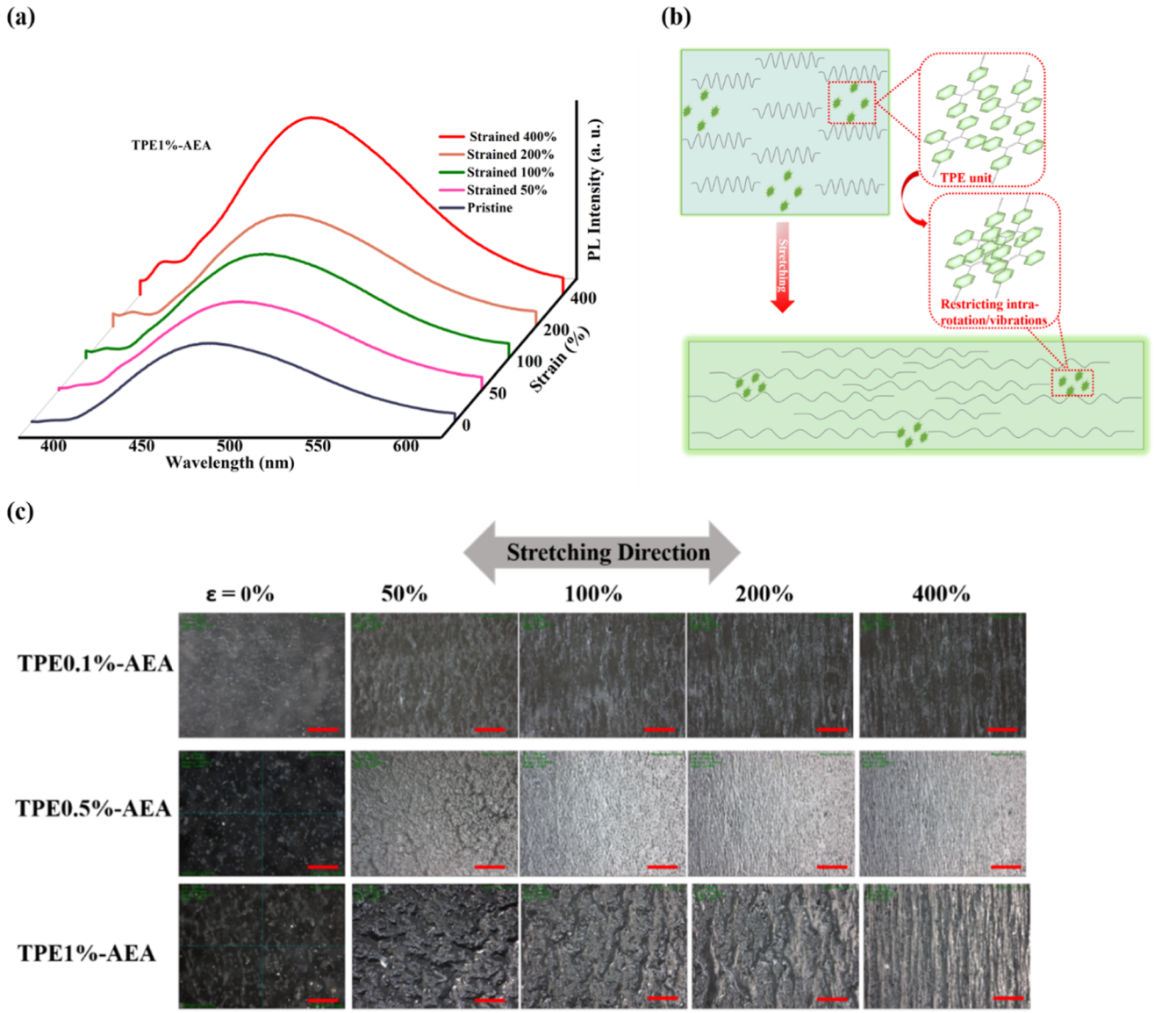


Figure 3. (a) PL spectra of the **TPE1%-AEA** elastomer at different strained states; (b) schematic diagram of the possible mechanism of stretch-dependent luminescence enhancement; and (c) optical microscopy images (the scale bar is 10 μm) of **TPE-AEA** elastomers upon applied strain from 0 to 400% strain.

elastomers are depicted in Figures S11−S13 respectively. After self-healing for 1 h, **TPE1%-AEA**, **TPE0.5%-AEA**, **TPE0.1%-AEA**, and **TPE0%-AEA** elastomers recovered the maximum stress−strain of 190, 240, 295, and 322%, respectively. The self-healing efficiencies for the corresponding samples were calculated to be 30, 36, 41, and 42%, respectively, indicating that the density of hydrogen bonds can increase the rate of self-healing. These elastomers exhibited time-dependent self-healing behaviors, where longer healing times resulted in higher fracture strain recovery. After 12 h of healing, the healed elastomer had an even higher stress−strain recovery rate, with a final self-healing efficiency of over 70%. Among all the elastomers, **TPE0%-AEA** without **TPE** units showed the highest self-healing efficiency of 81%, indicating that rigid TPE units sacrifice self-healing efficiency. In addition, X-ray diffraction (XRD) tests of all elastomers were recorded, as shown in Figure S14. XRD results show that all elastomers are amorphous before and after self-healing. The amorphous dynamic network structure facilitates the dissociation−association of hydrogen bonds during deformation or fracture. Generally, the completion of the self-healing process depends primarily on the reorganization of dynamic hydrogen bonds.[46,47] Detailed data of the mechanical properties are summarized in Table S1 in the Supporting Information.

To study the effect of the stretchability on the optical properties of AIE elastomers, PL spectra were obtained for all elastomers in the pristine, stretched 50, 100, 200, and 400% states. Taking **TPE1%-AEA** as a typical sample to investigate its emissive behavior under mechanical stretching (Figure 3a), the emissive intensity increased when these elastomers were subjected to mechanical stretching. Other AIE elastomers also exhibited similar behaviors (Figures S15, S16). The AIE nature of the TPE molecules is that their intramolecular rotations and vibrations are confined to the aggregated state, leading to the disappearance of these energy acceptors, which allows the retention of electron excitation energy.[48,49] When **TPE-AEA** elastomers containing AIE luminogens are stretched, the network structure becomes more compact, resulting in a

https://doi.org/10.1021/acs.macromol.3c00088
Macromolecules XXXX, XXX, XXX−XXX

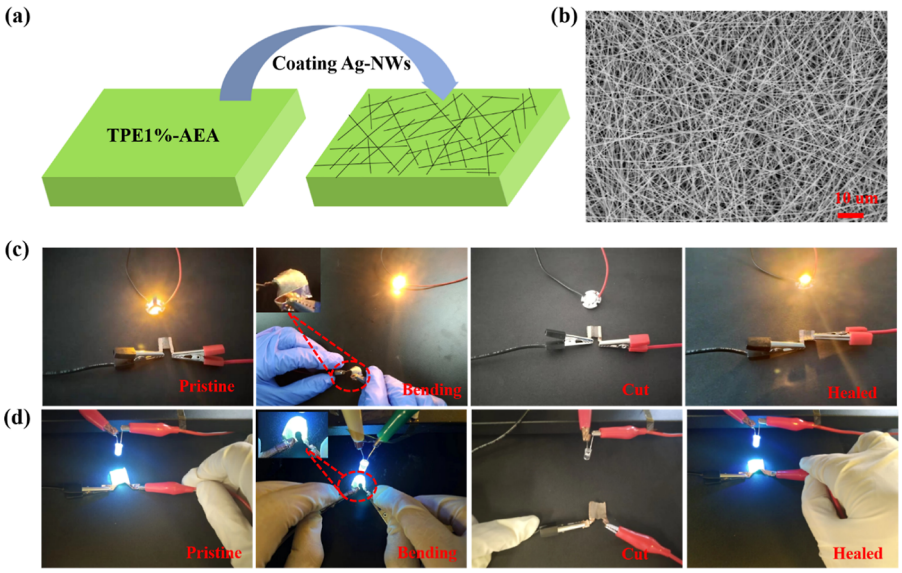


Figure 4. (a) Schematic diagram of the preparation of the self-healable conductor based on the **TPE1%-AEA** elastomer. (b) SEM image of the as-prepared self-healable conductor. (c) Demonstration of the healing process for the self-healable conductor with yellow LEDs at pristine, bending, cut, and healed states. (d) Demonstration of the smart luminous processes of the self-healable conductor.

reduction of the vibrational line domains around the TPE units. Such a more aggregated behavior restricts the intra-rotations and vibrations of the TPE molecules, leading to an increase in AIE intensity. Figure 3b depicts a possible mechanism for the stretch-induced luminescence enhancement. In general, the luminescence intensity of all elastomers showed a high tensile dependence during stretching, which revealed that the successful synthesis of the resulting elastomers did not sacrifice their photophysical properties including the high emission intensity even under straining. The resulting elastomers can retain a better luminescence than their original samples when stretched, indicating their significant potential for a variety of applications.

To gain deep insights into the morphology, all AIE elastomers were prepared for evaluation *via* an optical microscope upon straining from 0 to 400% (Figure 3c), which revealed a uniform distribution of the network and dynamic changes in surface morphology. Comparing these AIE elastomers with luminescence units of different molar ratios, the results show that the rigid TPE luminescent units affect the stretchability of the elastomers and produce a rougher surface in the non-stretched states. When these elastomers were stretched, **TPE1%-AEA** generated large cracks that went against energy dissipation, resulting in a decrease in stretchability. The higher soft side chains in the polymer lead to better stretchability. Meanwhile, the cross-linked network became more compact in the stretched states, resulting in a tighter stacking of the conjugated units. To investigate the physical characteristics of self-healing behaviors of the **TPE1%-AEA** elastomer, the self-healing process was measured using scanning electron microscopy (SEM). SEM images of **TPE1%-AEA** confirmed that the physical interface between the damaged surfaces was sufficiently healed that the gaps were indiscernible (Figure S17), confirming the self-healing process. The cross-sectional SEM image of **TPE1%-AEA** (Figure S18) also shows its homogeneous cross-linked network. According to surface and cross-sectional SEM images of the **TPE1%-AEA**, the AIE elastomer generated a cross-linked network system, resulting in a higher self-healing efficiency.

Owing to their excellent luminescence and stretchable self-healing properties, these elastomers can be used as substrates for attaching electronic devices onto soft surfaces, which holds great promise in optoelectronic devices. Flexible and autonomous self-healing electrodes composed of Ag nanowires (Ag-NWs) as the conductive layer and **TPE1%-AEA** as the supporting layer were fabricated. Ag-NWs were transferred onto the surface of the as-prepared **TPE1%-AEA** elastomer *via* classical vacuum filtration methods (Figure 4a).[50] According to the SEM image (Figure 4b), Ag-NWs with a length of 20 μm and a diameter of 30 nm were randomly distributed on the surface of the **TPE1%-AEA** elastomer in an interlaced pattern. The overlapping and connection among Ag-NWs lead to the high conductivity. To evaluate the electrical healing after damage, a voltage of 5 V was applied to the as-prepared conductor and connected to a yellow LED. As illustrated in Figure 4c, the LED is turned on and remains lit even under bending. Subsequently, the conductor was cut to break the circuit, and the lit LED was turned off immediately. In particular, the electrical conductivity of the sample could restore after bringing the two pieces together for 10 min. This was primarily ascribed to the self-healable capability of the underlying elastomer. Furthermore, to more directly compare the conductivity of the original and self-healing samples, the corresponding sheet resistances were assessed to be 1.01 and 1.14 Ω/sq, respectively. The recovery of electrical properties of the as-prepared conductor was accompanied by mechanical healing without external stimuli. Besides, the prepared conductor was connected to a 365 nm ultraviolet LED at a voltage of 5 V. As shown in Figure 4d, the conductor emitted when the 365 nm ultraviolet LED was lit at pristine, bending, and healed states. When the conductor was cut into halves, the circuit was broken and it was immediately quenched. The as-prepared conductor maintained luminous means the circuit of the optical device is operating. In short, the luminous conductor demonstrates a smart luminous process, which means that it is possible to detect whether a circuit is working by observing whether the luminous conductor is emitting light.

https://doi.org/10.1021/acs.macromol.3c00088
Macromolecules XXXX, XXX, XXX−XXX

In addition, an optoelectronic device based on the **TPE1%-AEA** elastomer was prepared to investigate its light-emitting properties. As shown in Figure S19, a 365 nm ultraviolet LED coated with the **TPE1%-AEA** film was fabricated and lit to show green light. It was then transferred to water for a period of time, exhibiting the blue−white color inherent to the ultraviolet LED. After removal from the water and drying, the LED regained its green light emission. The results can be attributed to the swelling effect of the **TPE1%-AEA** coating in water, disrupting the aggregation of TPE molecules, thus extinguishing its luminescence, and after drying, it returned to its aggregated state and emitted green light. These versatile features of the prepared elastomers can therefore offer a wide range of application possibilities.

CONCLUSIONS

In summary, this work presents a simple method to construct intrinsically stretchable and room-temperature self-healable luminescent materials with high solid-state quantum efficiency based on H-bond cross-linking networks. The as-prepared elastomers enable one to retain the intrinsic luminescent characteristics, meanwhile incorporating new mechanical properties by cross-linking non-conjugated chains with the H-bonding network. These elastomers exhibited low modulus, high tensile, and structural self-healing characteristics. Moreover, the structure of luminescent elastomers with cross-linked interactions of dynamic noncovalent H-bonding allows them to recover fluorescence responsiveness and self-healing capabilities after inevitable damages. The elastomers deposited with Ag-NWs layers can act as stretchable and self-healing conductors, which offers a novel approach to the development of future wearable electronics. The results shed light on the design and synthesis of stretchable and self-healable luminescent elastomers with high PLQYs, which are promising for broad applications in flexible and stretchable electronic devices.

ASSOCIATED CONTENT

Supporting Information

The Supporting Information is available free of charge at https://pubs.acs.org/doi/10.1021/acs.macromol.3c00088.

Experimental section including materials, instrumentation and characterization methods, and synthesis procedures; ^{1}H NMR spectra, FTIR spectra, UV−vis and fluorescence spectra, stress−strain curves, SEM images, and XRD results for the prepared elastomers (PDF)

AUTHOR INFORMATION

Corresponding Author

Wen-Yong Lai − *State Key Laboratory of Organic Electronics and Information Displays (SKLOEID), Institute of Advanced Materials (IAM), Nanjing University of Posts & Telecommunications, Nanjing 210023, China; Frontiers Science Center for Flexible Electronics (FSCFE), MIIT Key Laboratory of Flexible Electronics (KLoFE), Northwestern Polytechnical University, Xi'an 710072, China;* orcid.org/0000-0003-2381-1570; Email: iamwylai@njupt.edu.cn

Authors

Yi Wan − *State Key Laboratory of Organic Electronics and Information Displays (SKLOEID), Institute of Advanced Materials (IAM), Nanjing University of Posts & Telecommunications, Nanjing 210023, China*

Xiang-Chun Li − *State Key Laboratory of Organic Electronics and Information Displays (SKLOEID), Institute of Advanced Materials (IAM), Nanjing University of Posts & Telecommunications, Nanjing 210023, China*

Jin Chen − *State Key Laboratory of Organic Electronics and Information Displays (SKLOEID), Institute of Advanced Materials (IAM), Nanjing University of Posts & Telecommunications, Nanjing 210023, China*

Qian Wang − *State Key Laboratory of Organic Electronics and Information Displays (SKLOEID), Institute of Advanced Materials (IAM), Nanjing University of Posts & Telecommunications, Nanjing 210023, China*

Chen Liu − *State Key Laboratory of Organic Electronics and Information Displays (SKLOEID), Institute of Advanced Materials (IAM), Nanjing University of Posts & Telecommunications, Nanjing 210023, China;* orcid.org/0000-0002-2660-8116

Cheng-Fang Liu − *State Key Laboratory of Organic Electronics and Information Displays (SKLOEID), Institute of Advanced Materials (IAM), Nanjing University of Posts & Telecommunications, Nanjing 210023, China*

Complete contact information is available at: https://pubs.acs.org/10.1021/acs.macromol.3c00088

Author Contributions

[§]Y.W. and X.-C.L contributed equally.

Notes

The authors declare no competing financial interest.

ACKNOWLEDGMENTS

We acknowledge financial support from the National Natural Science Foundation of China (21835003, 21674050, 21422402, 62005126, and 61704077), the Natural Science Foundation of Jiangsu Province (BE2019120), the National Key Basic Research Program of China (2017YFB0404501, 2014CB648300), the China Postdoctoral Science Foundation (2019M650121, 2016M601784, 2017M620519, and 2017T100358), the Postdoctoral Science Foundation of Jiangsu Province (1701135B), Program for Jiangsu Specially Appointed Professor (RK030STP15001), the Six Talent Peaks Project of Jiangsu Province (TD-XCL-009), the 333 Project of Jiangsu Province (BRA2017402), the NUPT "1311 Project" and the NUPT Scientific Foundation (NY220152, NY218164, and NY217169), the State Key Laboratory of Organic Electronics and Information Displays (GZR2022010022), the Leading Talent of Technological Innovation of National Ten-Thousands Talents Program of China, the Excellent Scientific and Technological Innovative Teams of Jiangsu Higher Education Institutions (TJ217038), Innovation Project of Jiangsu Province (KYCX185_0850), the Synergetic Innovation Center for Organic Electronics and Information Displays, and the Priority Academic Program Development of Jiangsu Higher Education Institutions (PAPD).

REFERENCES

(1) Farinola, G. M.; Ragni, R. Electroluminescent materials for white organic light emitting diodes. *Chem. Soc. Rev.* **2011**, *40*, 3467−3482.
(2) Nakanotani, H.; Higuchi, T.; Furukawa, T.; Masui, K.; Morimoto, K.; Numata, M.; Tanaka, H.; Sagara, Y.; Yasuda, T.; Adachi, C. High-efficiency organic light-emitting diodes with fluorescent emitters. *Nat. Commun.* **2014**, *5*, 4016.

(3) Zhang, X.; Zhang, M.; Liu, M.; Chen, Y.; Wang, J.; Zhang, X.; Zhang, J.; Lai, W.-Y.; Huang, W. Highly efficient tandem organic light-emitting devices adopting a nondoped charge-generation unit and ultrathin emitting layers. *Org. Electron.* **2018**, *53*, 353−360.
(4) Zhang, Q.; Divayana, Y.; Xiao, J.; Wang, Z.; Tiekink, E.; Doung, H.; Zhang, H.; Boey, F.; Sun, X.; Wudl, F. Synthesis, characterization, and bipolar transporting behavior of a new twisted polycyclic aromatic hydrocarbon: 1′,4′-diphenyl-naphtho-(2′.3′:1.2)-pyrene-6′-nitro-7′-methyl carboxylate. *Chem. Eur J.* **2010**, *16*, 7422−7426.
(5) Kuehne, A. J.; Gather, M. C. Organic lasers: recent developments on materials, device geometries, and fabrication techniques. *Chem. Rev.* **2016**, *116*, 12823−12864.
(6) Liu, C.-F.; Sang, M.; Lai, W.-Y.; Lu, T. T.; Liu, X.; Huang, W. Design and synthesis of monodisperse macromolecular starbursts based on a triazine center with multibranched oligofluorenes as efficient gain media for organic lasers. *Macromolecules* **2018**, *51*, 1325−1335.
(7) Jiang, Y.; Liu, Y.-Y.; Liu, X.; Lin, H.; Gao, K.; Lai, W.-Y.; Huang, W. Organic solid-state lasers: A materials view and future development. *Chem. Soc. Rev.* **2020**, *49*, 5885−5944.
(8) Wang, F.; Li, X.-C.; Lai, W.-Y.; Chen, Y.; Huang, W.; Wudl, F. Synthesis and characterization of symmetric cyclooctatetraindoles: exploring the potential as electron-rich skeletons with extended π-systems. *Org. Lett.* **2014**, *16*, 2942−2945.
(9) Zhang, L.; Liu, X. A.; Gillis, K. D.; Glass, T. E. A high-affinity fluorescent sensor for catecholamine: application to monitoring norepinephrine exocytosis. *Angew. Chem.* **2019**, *131*, 7693−7696.
(10) Wang, T.; Zhang, N.; Bai, W.; Bao, Y. Fluorescent chemosensors based on conjugated polymers with N-heterocyclic moieties: two decades of progress. *Polym. Chem.* **2020**, *11*, 3095−3114.
(11) Han, T.-H.; Lee, Y.; Choi, M.-R.; Woo, S.-H.; Bae, S.-H.; Hong, B. H.; Ahn, J.-H.; Lee, T.-W. Extremely efficient flexible organic light-emitting diodes with modified graphene anode. *Nat. Photonics* **2012**, *6*, 105−110.
(12) Ostroverkhova, O. Organic optoelectronic materials: mechanisms and applications. *Chem. Rev.* **2016**, *116*, 13279−13412.
(13) Im, Y.; Byun, S. Y.; Kim, J. H.; Lee, D. R.; Oh, C. S.; Yook, K. S.; Lee, J. Y. Recent progress in high-efficiency blue-light-emitting materials for organic light-emitting diodes. *Adv. Funct. Mater.* **2017**, *27*, 1603007.
(14) Tuong Ly, K.; Chen-Cheng, R.-W.; Lin, H.-W.; Shiau, Y.-J.; Liu, S.-H.; Chou, P.-T.; Tsao, C.-S.; Huang, Y.-C.; Chi, Y. Near-infrared organic light-emitting diodes with very high external quantum efficiency and radiance. *Nat. Photonics* **2017**, *11*, 63−68.
(15) Li, Q.; Li, Z. Molecular packing: another key point for the performance of organic and polymeric optoelectronic materials. *Acc. Chem. Res.* **2020**, *53*, 962−973.
(16) Xiao, J.; Yang, H.; Yin, Z.; Guo, J.; Boey, F.; Zhang, H.; Zhang, Q. Preparation, characterization, and photoswitching/light-emitting behaviors of coronene nanowires. *J. Mater. Chem.* **2011**, *21*, 1423−1427.
(17) Luo, C. S.; Wan, P.; Yang, H.; Shah, S. A. A.; Chen, X. Healable transparent electronic devices. *Adv. Funct. Mater.* **2017**, *27*, 1606339.
(18) Qian, Y.; Zhang, X.; Xie, L.; Qi, D.; Chandran, B. K.; Chen, X.; Huang, W. Stretchable organic semiconductor devices. *Adv. Mater.* **2016**, *28*, 9243−9265.
(19) Au-Duong, A.-N.; Wu, C.-C.; Li, Y.-T.; Huang, Y.-S.; Cai, H.-Y.; Jo Hai, I.; Cheng, Y.-H.; Hu, C.-C.; Lai, J.-Y.; Kuo, C.-C.; et al. Synthetic concept of intrinsically elastic luminescent polyfluorene-based copolymers via RAFT polymerization. *Macromolecules* **2020**, *53*, 4030−4037.
(20) Tan, Y. J.; Wu, J.; Li, H.; Tee, B. C. K. Self-healing electronic materials for a smart and sustainable future. *ACS Appl. Mater. Interfaces* **2018**, *10*, 15331−15345.
(21) Oh, J. Y.; Rondeau-Gagné, S.; Chiu, Y.-C.; Chortos, A.; Lissel, F.; Wang, G.-J. N.; Schroeder, B. C.; Kurosawa, T.; Lopez, J.; Katsumata, T.; et al. Intrinsically stretchable and healable semiconducting polymer for organic transistors. *Nature* **2016**, *539*, 411−415.
(22) Zhang, K.; Deng, Y.; Shi, X.; Li, X.; Qi, D.; Jiang, B.; Huang, Y. Interface chelation induced by pyridine-based polymer for efficient and durable air-processed perovskite solar cells. *Angew. Chem., Int. Ed.* **2022**, *61*, No. e202112673.
(23) He, C. L.; Liang, F. C.; Veeramuthu, L.; Cho, C. J.; Benas, J. S.; Tzeng, Y. R.; Tseng, Y. L.; Chen, W. C.; Rwei, A.; Kuo, C. C. Super tough and spontaneous water-assisted autonomous self-healing elastomer for underwater wearable electronics. *Adv. Sci.* **2021**, *8*, 2102275.
(24) Liu, G.; Liu, J.; Ye, X.; Nie, L.; Gu, P.; Tao, X.; Zhang, Q. Self-healing behavior in a thermo-mechanically responsive cocrystal during a reversible phase transition. *Angew. Chem.* **2017**, *129*, 204−208.
(25) Kang, J.; Son, D. H.; Wang, G. N.; Liu, Y.; Lopez, J.; Kim, Y.; Oh, J. Y.; Katsumata, T.; Mun, J.; Lee, Y.; et al. Tough and water-insensitive self-healing elastomer for robust electronic skin. *Adv. Mater.* **2018**, *30*, 1706846.
(26) Jiang, C.; Zhang, L.; Yang, Q.; Huang, S.; Shi, H.; Long, Q.; Qian, B.; Liu, Z.; Guan, Q.; Liu, M.; et al. Self-healing polyurethane-elastomer with mechanical tunability for multiple biomedical applications in vivo. *Nat. Commun.* **2021**, *12*, 4395.
(27) Wang, W.; Zhang, W.; Liu, Z.; Xue, Y.; Lei, X.; Gong, G.; Zhang, Q. Towards a tough reprocessable and self-healable acrylonitrile-butadiene rubber based on strong hydrogen bonding interactions. *J. Mater. Chem. C* **2021**, *9*, 6241−6250.
(28) Rao, Y.-L.; Chortos, A.; Pfattner, R.; Lissel, F.; Chiu, Y.-C.; Feig, V.; Xu, J.; Kurosawa, T.; Gu, X.; Wang, C.; et al. Stretchable self-healing polymeric dielectrics cross-linked through metal−ligand coordination. *J. Am. Chem. Soc.* **2016**, *138*, 6020−6027.
(29) Li, C.-H.; Wang, C.; Keplinger, C.; Zuo, J.-L.; Jin, L.; Sun, Y.; Zheng, P.; Cao, Y.; Lissel, F.; Linder, C.; et al. A highly stretchable autonomous self-healing elastomer. *Nat. Chem.* **2016**, *8*, 618−624.
(30) Tian, M.; Zuo, H.; Wang, J.; Ning, N.; Yu, B.; Zhang, L. A silicone elastomer with optimized and tunable mechanical strength and self-healing ability based on strong and weak coordination bonds. *Polym. Chem.* **2020**, *11*, 4047−4057.
(31) Das, A.; Sallat, A.; Böhme, F.; Suckow, M.; Basu, D.; Wießner, S.; Stöckelhuber, K. W.; Voit, B.; Heinrich, G. Ionic modification turns commercial rubber into a self-healing material. *ACS Appl. Mater. Interfaces* **2015**, *7*, 20623−20630.
(32) Miwa, Y.; Kurachi, J.; Kohbara, Y.; Kutsumizu, S. Dynamic ionic crosslinks enable high strength and ultrastretchability in a single elastomer. *Commun. Chem.* **2018**, *1*, 5.
(33) Xu, C.; Cao, L.; Lin, B.; Liang, X.; Chen, Y. Design of self-healing supramolecular rubbers by introducing ionic cross-links into natural rubber via a controlled vulcanization. *ACS Appl. Mater. Interfaces* **2016**, *8*, 17728−17737.
(34) Liu, J.; Tan, C. S. Y.; Yu, Z.; Li, N.; Abell, C.; Scherman, O. A. Tough supramolecular polymer networks with extreme stretchability and fast room-temperature self-healing. *Adv. Mater.* **2017**, *29*, 1605325.
(35) Xiao, L.; Shi, J.; Wu, K.; Lu, M. Self-healing supramolecular waterborne polyurethane based on host−guest interactions and multiple hydrogen bonds. *React. Funct. Polym.* **2020**, *148*, 104482.
(36) Urban, M. W.; Davydovich, D.; Yang, Y.; Demir, T.; Zhang, Y.; Casabianca, L. Key-and-lock commodity self-healing copolymers. *Science* **2018**, *362*, 220−225.
(37) Mei, J. F.; Jia, X. Y.; Lai, J. C.; Sun, Y.; Li, C. H.; Wu, J. H.; Cao, Y.; You, X. Z.; Bao, Z. A highly stretchable and autonomous self-healing polymer based on combination of pt··· pt and π−π interactions. *Macromol. Rapid Commun.* **2016**, *37*, 1667−1675.
(38) Kim, S. M.; Jeon, H.; Shin, S. H.; Park, S. A.; Jegal, J.; Hwang, S. Y.; Oh, D. X.; Park, J. Superior toughness and fast self-healing at room temperature engineered by transparent elastomers. *Adv. Mater.* **2018**, *30*, 1705145.
(39) Zhang, B.; Zhang, P.; Zhang, H.; Yan, C.; Zheng, Z.; Wu, B.; Yu, Y. A transparent, highly stretchable, autonomous self-healing

https://doi.org/10.1021/acs.macromol.3c00088
Macromolecules XXXX, XXX, XXX−XXX

poly(dimethyl siloxane) elastomer. *Macromol. Rapid Commun.* **2017**, *38*, 1700110.
(40) Ying, H.; Zhang, Y.; Cheng, J. Dynamic urea bond for the design of reversible and self-healing polymers. *Nat. Commun.* **2014**, *5*, 3218.
(41) Yang, J.; Zhang, Z.; Yan, Y.; Liu, S.; Li, Z.; Wang, Y.; Li, H. Highly stretchable and fast self-healing luminescent materials. *ACS Appl. Mater. Interfaces* **2020**, *12*, 13239−13247.
(42) Kokado, K.; Sada, K. Consideration of molecular structure in the excited state to design new luminogens with aggregation-induced emission. *Angew. Chem., Int. Ed.* **2019**, *58*, 8632−8639.
(43) Yang, Z.; Chi, Z.; Mao, Z.; Zhang, Y.; Liu, S.; Zhao, J.; Aldred, M. P.; Chi, Z. Recent advances in mechano-responsive luminescence of tetraphenylethylene derivatives with aggregation-induced emission properties. *Mater. Chem. Front.* **2018**, *2*, 861−890.
(44) Khajehsaeid, H.; Arghavani, J.; Naghdabadi, R. A hyperelastic constitutive model for rubber-like materials. *Eur J Mech A Solids* **2013**, *38*, 144−151.
(45) Beda, T. An approach for hyperelastic model-building and parameters estimation a review of constitutive models. *Eur. Polym. J.* **2014**, *50*, 97−108.
(46) Guo, M.; Pitet, L. M.; Wyss, H. M.; Vos, M.; Dankers, P. Y. W.; Meijer, E. W. Tough stimuli-responsive supramolecular hydrogels with hydrogen-bonding network junctions. *J. Am. Chem. Soc.* **2014**, *136*, 6969−6977.
(47) Wang, C.; Liu, N.; Allen, R.; Tok, J. B. H.; Wu, Y.; Zhang, F.; Chen, Y.; Bao, Z. A rapid and efficient self-healing thermo-reversible elastomer crosslinked with graphene oxide. *Adv. Mater.* **2013**, *25*, 5785−5790.
(48) Liu, J.; Zhang, H.; Hu, L.; Wang, J.; Lam, J. W.; Blancafort, L.; Tang, B. Z. Through-space interaction of tetraphenylethylene: what, where, and how. *J. Am. Chem. Soc.* **2022**, *144*, 7901−7910.
(49) Mei, J.; Leung, N. L.; Kwok, R. T.; Lam, J. W.; Tang, B. Z. Aggregation-induced emission: together we shine, united we soar. *Chem. Rev.* **2015**, *115*, 11718−11940.
(50) Madaria, A. R.; Kumar, A.; Ishikawa, F. N.; Zhou, C. Uniform, highly conductive, and patterned transparent films of a percolating silver nanowire network on rigid and flexible substrates using a dry transfer technique. *Nano Res.* **2010**, *3*, 564−573.

https://doi.org/10.1021/acs.macromol.3c00088
Macromolecules XXXX, XXX, XXX−XXX